Joint Pathology Center
Veterinary Pathology Services

WEDNESDAY SLIDE CONFERENCE 2019-2020

Conference 12

11 December 2019

CASE I: MSKCC/WMC/RU HB (JPC 4032968).

Signalment: Young adult, intact female Syrian hamster (*Mesocricetus auratus*)

History: Both animals are from the same group of eight hamsters that were shipped together three weeks prior to being experimentally inoculated with *Leishmania donovani*. All animals were administered intraperitoneal preparations of *Leishmania* derived from tissue homogenates of previously infected hamsters. Shortly after treatment, seven of the eight animals became acutely lethargic and dehydrated with perineal staining. Multiple animals were found dead and the remainder with euthanized as clinical signs progressed.

Gross Pathology: The abdomen is moderately distended and there is mild perineal fecal staining.

Approximately 1-2ml of slightly turbid, serosanguinous fluid is present within the abdominal cavity. The mesentery is markedly thickened and diffusely white. Intestinal loops are firmly adhered to one another by mesenteric adipose tissue which

Viscera, hamster: A single mass incorporates much of the abdominal viscera, including the liver, spleen, multiple loops of gut, and mesentery. (Photo courtesy of: Memorial Sloan-Kettering Cancer Center, 1275 York Ave, New York, New York, 10065, http://www.mskcc.org/research/comparative-medicine-pathology).

envelopes the spleen and uterus, and is adhered to the visceral surface of the liver. Mesenteric lymph nodes are enlarged and poorly demarcated, blending into the surrounding mesentery. The cecum is moderately distended by feed material and the distal colon is empty.

The liver is enlarged (10.6% of bodyweight) with rounded margins, and is diffusely pale tan and friable with an enhanced reticular

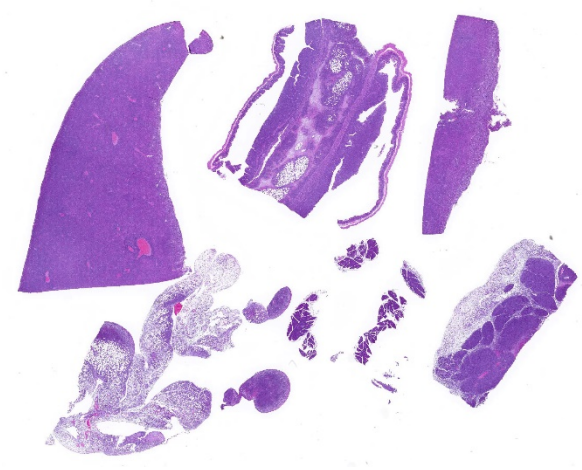

Viscera, hamster: Sections of liver, omentum, and pancreas are all infiltrated by a densely cellular neoplasm. (HE, 9X)

pattern. The kidneys are mildly enlarged, pale tan and swollen. The pancreas and peripancreatic adipose tissue are mottled tan to red and firm.

In the right cranial lobe of the lung, there was a firm, poorly demarcated structure palpable in the parenchyma. On the serosal surface of the left middle lobe, there were multiple plaque-like, sharply circumscribed, brown depositions of material observed (histologically identified as multifocal calcifications of pulmonary basal membranes with reactive histiocytic inflammation).

Laboratory results:

Cytology of the abdominal fluid revealed moderate numbers of small to medium sized lymphocytes, fewer large round cells, and small numbers of mesothelial cells and macrophages. Impression smears of the liver were highly cellular and composed predominantly of large round cells, approximately 10-20um in diameter, with a high nuclear to cytoplasmic ratio, large round nucleus, finely clumped chromatin, multiple nucleoli, and a small amount of basophilic cytoplasm.

Microscopic Description:

Mesentery including mesenteric lymph nodes, spleen and pancreas (variably includes small intestine): A poorly demarcated neoplastic infiltrate dissects throughout the mesentery which is extensively adhered to the splenic capsule, pancreas, mesenteric lymph nodes and intestinal serosa. Neoplastic round cells are arranged into densely cellular, unencapsulated sheets that variably efface the splenic and lymph node parenchyma and extensively disrupt the small intestinal muscularis and mucosa. Neoplastic cells have indistinct margins, a moderate amount of amphophilic cytoplasm and 10-15um diameter, round nuclei with coarsely stippled chromatin and variably conspicuous nucleoli. Frequent cells are necrotic and tingible body macrophages are scattered throughout the infiltrate. Anisocytosis and anisokaryosis are moderate and up to 7 mitotic figures are present per high power field (x400). Large areas of acute coagulative necrosis are scattered throughout mesenteric lymph nodes, variably accompanied by aggregates of fragmented mineral material (dystrophic mineralization). Scattered macrophages in remnant subcapsular sinuses and at the margins of necrotic foci contain dozens of oval-shaped, 2-3um diameter, intracytoplasmic protozoa with a 1-2um, basophilic nucleus and a variably distinct, perpendicular kinetoplast (*Leishmania* amastigotes).

Liver: An intense neoplastic infiltrate diffusely percolates throughout hepatic sinusoids, disrupting hepatic cords, obscuring portal tracts and lining the tunica intima of frequent central veins. Frequent hepatocytes are dissociated with hypereosinophilic cytoplasm and pyknotic nuclei (necrosis).

Contributor's Morphologic Diagnosis:

Mesentery including mesenteric lymph nodes, spleen, pancreas and small intestine: Lymphoma

Mesenteric lymph nodes: Severe, acute, multifocal to coalescing, necrotizing splenitis with intrahistiocytic protozoa, etiology consistent with *Leishmania* sp.

Contributor's Comment All eight hamsters received intraperitoneal preparations of *Leishmania donovani* derived from tissue homogenates of previously infected animals. Within three weeks, all animals became acutely lethargic and dehydrated or died acutely. Gross and histologic findings were similar in all animals, which were characterized by intense mesenteric infiltrates of neoplastic round cells. The histologic appearance of neoplastic cells is most consistent with lymphoma. Consistent with the experimental history, scattered macrophages located at the margins of necrotic foci within the mesenteric lymph nodes contained cytoplasmic amastigotes. All animals were inoculated with *L. donovani* as part of a study investigating host immunoregulation of visceral leishmaniasis.

Protozoa of the family Trypanasomatidae, genus *Leishmania* cause a spectrum of disease in people ranging from subclinical infection to severe, disseminated cutaneous, mucocutaneous and visceral disease. Visceral leishmaniasis (VL) is the most severe form of disease and may be fatal. *Leishmania donovani* is the predominant cause of VL in East Africa and India, whereas *L. infantum* and *L. chagasi* predominate in the Mediterranean and Latin America, respectively.[1] The domestic dog is an important reservoir host for the latter two species. Humans are the only known reservoir of *L. donovani.*

Leishmania sp. proliferate in the midgut of phlebotomine sandflies where the flagellated leptomonad form appears as a leaf-shaped promastigote.[5] Upon transmission to mammalian hosts, the organism assumes the aflagellated, obligate intracellular leishmanial form, or amastigote, which proliferates within macrophages and dendritic cells of susceptible hosts. These are approximately 2um diameter with a basophilic nucleus and perpendicularly oriented kinetoplast.

Host susceptibility to clinical disease relates to the *Leishmania* species involved and individual host factors such as immunocompetence. In susceptible hosts, VL may cause persistent fever, leukopenia, hypergammaglobulinemia and hepatosplenomegaly. Chronic immune-complex deposition may result in glomerulonephritis in people. Clinical and pathologic findings are similar in dogs, consisting predominantly of hepatic granulomas, splenomegaly and lymphadenopathy.[5]

The Syrian hamster is a widely used experimental model of VL, developing clinical signs and lesions that recapitulate human and canine disease including splenic lymphoid depletion, hepatic granulomas and amyloid deposition within the spleen and liver.[1] Glomerulonephritis and inflammatory myopathies have also been reported. Despite developing clinical disease and lesions that closely approximate human VL, a lack of reagents and a poor immune response to infection are limiting factors in the Syrian hamster model, particularly for evaluation of vaccination strategies. Murine models have also been utilized to identify genes that play an important role in the pathogenesis of VL. In some mouse strains (eg. CBA) genetic resistance is conferred by the gene *Slc11a1*, which encodes a phagosomal membrane protein that limits intracellular *Leishmania* multiplication by Fe^{2+} deprivation.[1] Susceptible mouse strains (eg. BALB/c, C57BL/6) with impaired *Slc11a1* expression are susceptible to *Leishmania*; however, even susceptible mice typically overcome visceral infection.

Given the severity of the neoplastic infiltrate in all animals, the cause of death in these animals was determined to be lymphoma, rather than visceral leishmaniasis. Outbreaks of transmissible lymphoma due to *hamster polyomavirus* (HaPV) infection have been reported in hamster colonies causing lymphoma epizootics that affect up to 80% of young, naïve animals.[2] HaPV was initially described in association with epitheliomas in older hamsters.[3] Tumors arise from the epithelium of the hair follicle forming keratin-filled, cystic masses. Large

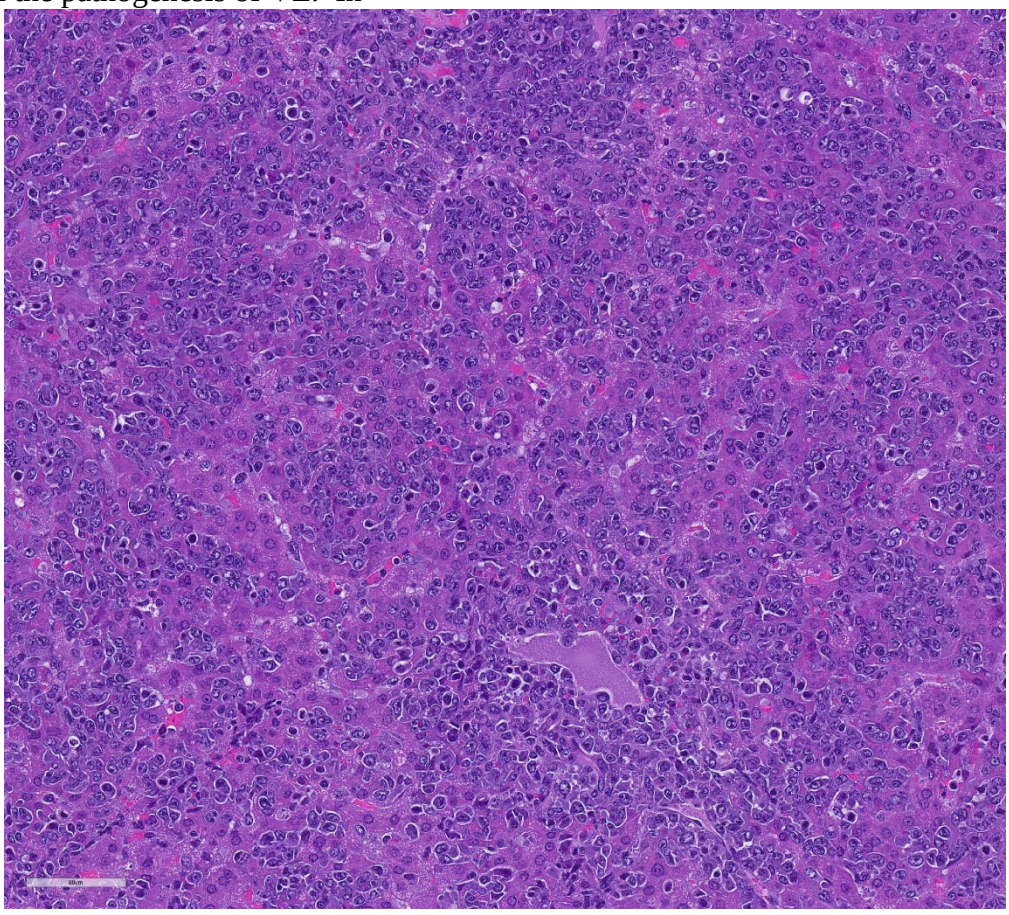

Liver, hamster: The liver is diffusely infiltrated by neoplastic lymphocytes which efface its normal sinusoidal pattern. (HE, 279X)

numbers of virus particles are detectable in keratinizing cells of epitheliomas. This contrasts with HaPV-associated lymphomas, which do not contain infectious virus, although thousands of copies of extrachromosomal viral DNA are present within neoplastic cells. Ha-PV associated lymphoma typically arises in the mesentery with infiltration of the liver, kidney, thymus, and other viscera. Tumors are usually lymphoid, although erythroblastic, myeloid and reticulosarcomatous forms may occur[3]. In enzootically infected, older hamsters the virus persists subclinically in the kidneys with intermittent shedding in urine.

In this case HaPV infection was suspected based on the clinical presentation but could not be confirmed by PCR (IDEXX RADIL). Lymphoma is rare in young hamsters and the rapid neoplastic progression in this group is highly suggestive of epizootic HaPV.[2] Ultrastructural imaging was not pursued as virus particles are not typically present in neoplastic lymphocytes.

It is unclear whether affected animals developed lymphoma prior to arrival at our facility or whether intraperitoneal *Leishmania* inoculation was the source of the tumor. It is possible that the tissue homogenate from which the inoculum was derived was infected with HaPV. It is also possible although somewhat less likely, that the donor animal had spontaneous lymphoma that was then transmitted to subsequent animals in the tissue homogenate. Transmissible tumors in the dog (canine transmissible venereal tumor) and Tasmanian devil (devil facial tumor disease) are associated with downregulation of tumor cell MHC expression, allowing successful allograft and proliferation in

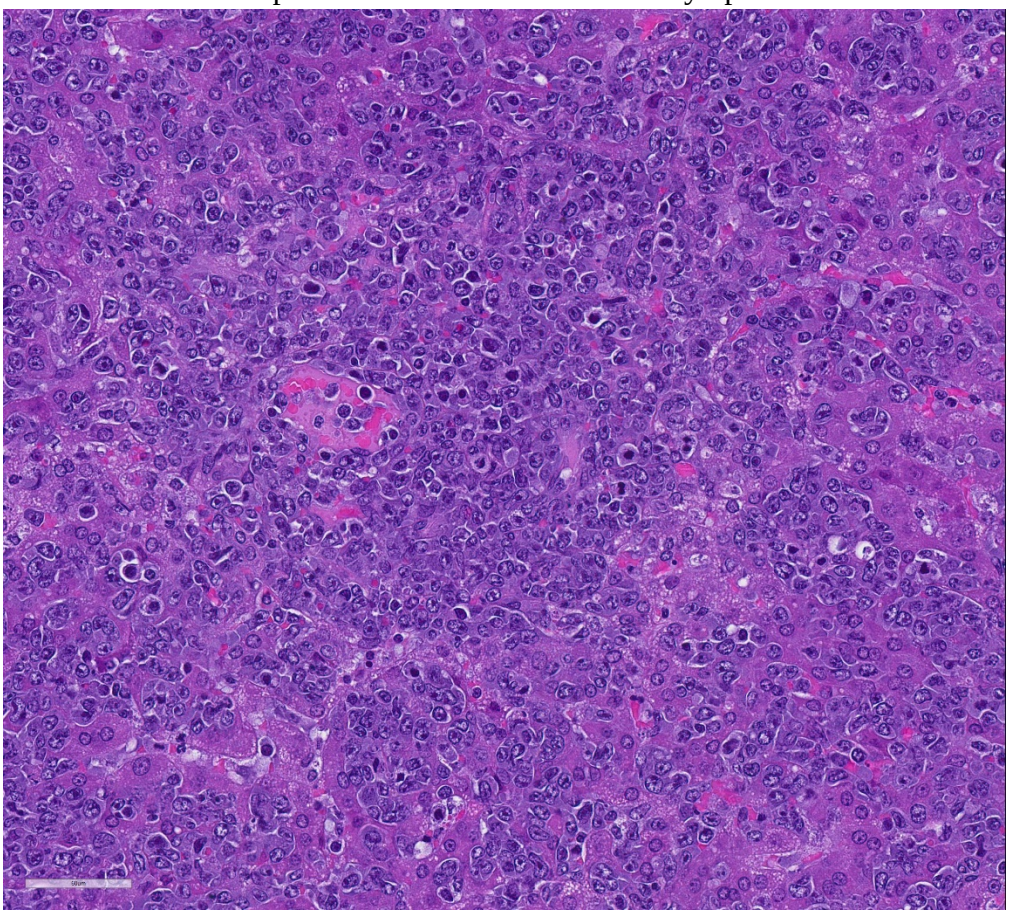

Liver, hamster: High magnification of the field in 1-3, demonstrating the large size of the neoplastic cells, abundant granular basophilic cytoplasm and high mitotic rate. (HE, 315X)

the absence of a host immune response.[4]

Contributing Institution:

Memorial Sloan-Kettering Cancer Center
1275 York Ave
New York, New York, 10065
http://www.mskcc.org/research/comparative-medicine-pathology

JPC Diagnosis: 1. Liver, spleen, omentum, pancreas: Lymphoma.
2. Liver, spleen, omentum, pancreas, macrophages: Intracytoplasmic amastigotes, rare.

JPC Comment: The contributor has provided an excellent review of leishmaniasis as well as the use of the Syrian hamster as the animal model for its visceral

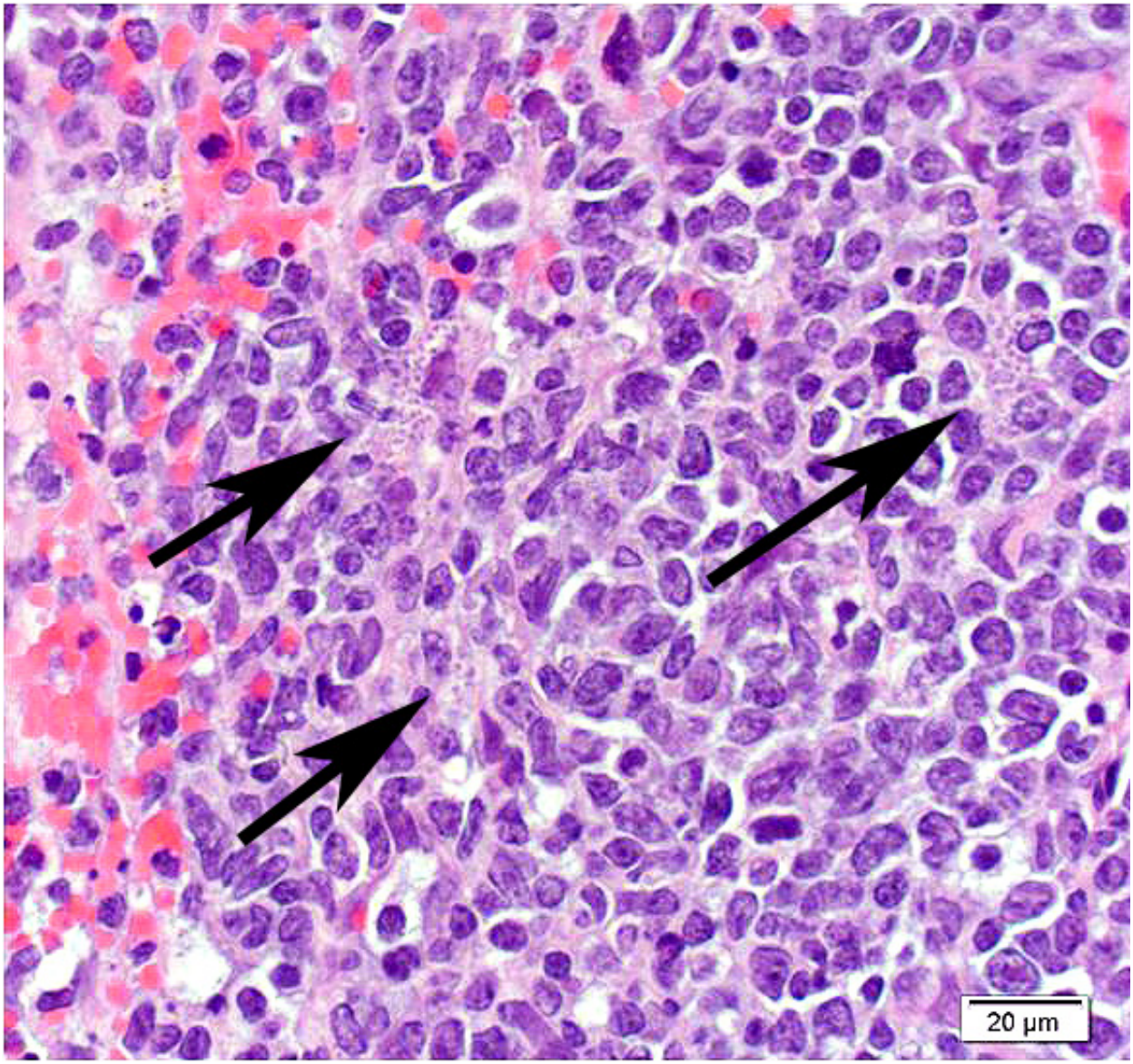

Spleen, hamster. Macrophages contain multiple intracytoplasmic amastigotes. (HE, 400X).

form. *Leishmania* has appeared multiple times in the Wednesday Slide Conference in the dog (WSC 2015-2016, Conf 17, Case 3, WSC 2013-2014 Conf 3, Case 3, WSC 2009-2010, Conf 13, Case 4, @WC 2007-2008, Conference 5, case 2). It has appeared twice in the hamster (WSC 1998-1999, Conf 10, Case 2 and WSC 1971-1972, Conference 22, case 2). The reader is directed to the comments on these cases for additional information.

The history of leishmaniasis is an ancient one, with identification of *Paleoleishmania* in fossilized form within the proboscis and gut of 100-million-year-old fly preserved in amber. Written records of cutaneous leishmaniasis begin in Assyrian tables describing "oriental sore", and *Leishmania* DNA has been recovered from Egyptian and Peruvian mummies. Evidence for immunization agains Leishmania dates back to ancient Arabia, whose physicians vaccinated children with exudate from the sores of active lesions or exposed them to sand flies to prevent the occurrence of disfiguring facial scars. Numerous reports in more modern times of "Allepo", "Jericho" and "Baghdad boil" are present in Middle Eastern literature, and numerous reports from explorers of the New World, including Francisco Pisarro described a similar scarring condition. Visceral leishmaniasis, or kala-azar, was first described by military surgeon Willian Twining in 1827 in India. Scottish pathologist William Boog Leishman was the first to observe and describe the amastigotes of *Leishmania* in autopsy of soldiers in India as well as infected rats. Weeks later, an Irish pathologist working at Madras veterinary college identified similar structures in Inidan subjects with splenomegaly and recurring fever. In 1903, Dr. William Ross identified the structures first described by Leishman and Donovan as a new species and not a degenerate trypanosome or piroplasm (as was currently thought at the time) and named the agent *Leishmania donovani*.

Currently visceral leishmaniasis remains a significant problem in 14 high-risk tropical countries, but numbers of cases, especially in India, appear to be on the decline. International travel and international transport of blood products (blood is not routinely checked for anti-leishmanial antibodies) has resulted in cases of VL in non-endemic countries. Ongoing instability in the Middle East and refugee crises also helps to import cutaneous forms of leishmaniasis into areas where it formerly was at a very low level.

Unfortunately, in the submitted sections, the changes associated with visceral leishmaniasis are greatly overshadowed by the large cell lymphoma presuably resulting from activation of hamster polyomavirus. Few of the participants noticed the presence of amastigotes within macrophages, as amastigote-laden macrophages were often overshadowed by the profound neoplastic infiltrate and the scattered apoptotic cells contained within.

References:

1. Nieto A *et al*. Mechanisms of resistance and susceptibility to experimental visceral leishmaniosis: BALB/c mouse versus syrian

hamster model. *Vet Res*. 2011;42(1):39

2. Percy DH and Barthold SW; Hamster. In: Pathology of Laboratory Rodents and Rabbits, Eds. Percy DH and Barthold SW, 3rd ed. pp181-183. , Wiley-Blackwell, Ames, IA, 2007
3. Scherneck S, Ulrich R and Feunteun J. The hamster polyomavirus--a brief review of recent knowledge. *Virus Genes*. 2001;22(1):93-101
4. Siddle HV et al. Reversible epigenetic down-regulation of MHC molecules by devil facial tumour disease illustrates immune escape by a contagious cancer. *Proc Natl Acad Sci U S A*. 2013;110(13):5103-8
5. Steverding D. The history of leishmaniasis. *Parasit Vect* 2017; (10):82-89.
6. Valli V; Hematopoietic System. In: Jubb, Kennedy & Palmer's Pathology of Domestic Animals, Ed. Maxie GM, 5th ed., pp.302-304, Saunders Elsevier, Philadelphia, PA, 2007

CASE II: A12-357 (JPC 4031109).

Signalment: 4 year old male rhesus macaque (*Macaca mulatta*).

History: This rhesus macaque was inoculated with SIVsmE6601:1 as part of a research study. Six months post inoculation, the animal was noted to have poor appetite and acute weight loss (18% body weight over 2 weeks). Clinical examination two days prior to euthanasia revealed severe respiratory distress with nasal discharge and wheezing, along with liquid diarrhea and a severe neutrophilic leukocytosis. Due to poor prognosis and progression towards simian acquired immunodeficiency syndrome, the animal was humanely euthanized.

Gross Pathology: The animal was in poor body condition with no appreciable body fat. The mucosa of the stomach was thickened and edematous. The duodenum was diffusely hyperemic. The liver and kidneys had pale foci scattered throughout the parenchyma extending through cut sections. All lung lobes were diffusely reddened and severely mottled dark red or pale brown and markedly thickened and firm.

Laboratory results: N/A

Microscopic Description:

Lung: Primarily focused around bronchi and bronchioles and involving approximately 40% of the tissue examined, alveolar spaces are filled with inflammatory cells consisting of neutrophils, epithelioid macrophages, and multinucleated giant cells admixed with edema, fibrin, cellular and karyorrhectic

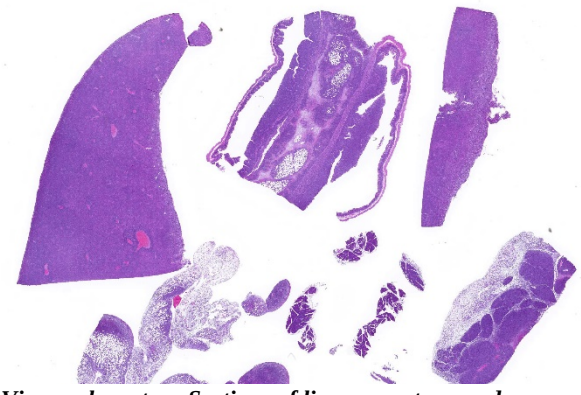

Viscera, hamster: Sections of liver, omentum, and pancreas are all infiltrated by a densely cellular neoplasm. (HE, 9X)

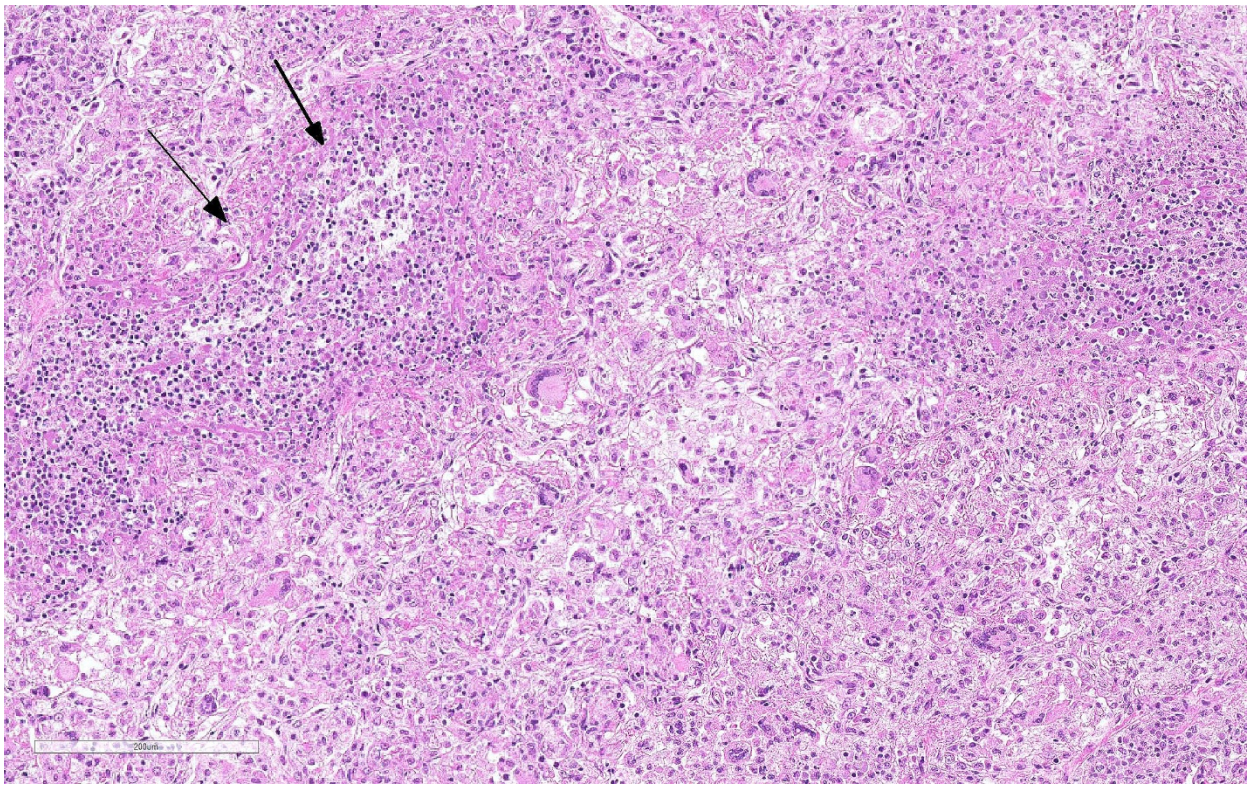

Lung, rhesus. Alveolar architecture is obscured by a mixed cellular infiltrate containing numerous macrophages, neutrophils and multinucleated viral syncytia. Airways are effaced as well (arrows). (HE, 276X)

debris, and extravasated red blood cells. Within several areas of inflammation are bacterial colonies (not present on each slide). The lumina of several bronchioles are partially occluded by neutrophils, histiocytes, cellular and karyorrhectic debris, and fibrin. Multifocally within alveolar spaces, are aggregations of foamy, eosinophilic fungal organisms (*Pneumocystis carinii*).

Contributor's Morphologic Diagnosis:

Lung: Multifocal, severe, chronic bronchointerstitial pneumonia with SIV giant cells and *Pneumocystis carinii*

Contributor's Comment Lentiviruses are a subfamily of retroviruses and include human immunodeficiency virus (HIV), simian immunodeficiency virus (SIV), equine infectious anemia virus (EIAV), ovine lentivirus (OvLV), bovine immunodeficiency virus, and feline immunodeficiency virus (FIV). Lentiviruses cause chronic disease syndromes including immunodeficiency, encephalitis, pneumonia, arthritis, anemia, thrombocytopenia, and lymphoid hyperplasia. SIV has proven a useful model to study HIV pathogenesis, as the virus is morphologically identical to HIV by electron microscopy, serologically related to HIV, and cytopathic for $CD4^+$ T cells.[7] SIV infected macaques develop peripheral lymphadenopathy, splenomegaly, diarrhea, weight loss, skin rash, pneumonia, septicemia, and hemogram abnormalities including leukopenia, lymphopenia, neutropenia, anemia, and thrombocytopenia. The appearance of multinucleate giant cells

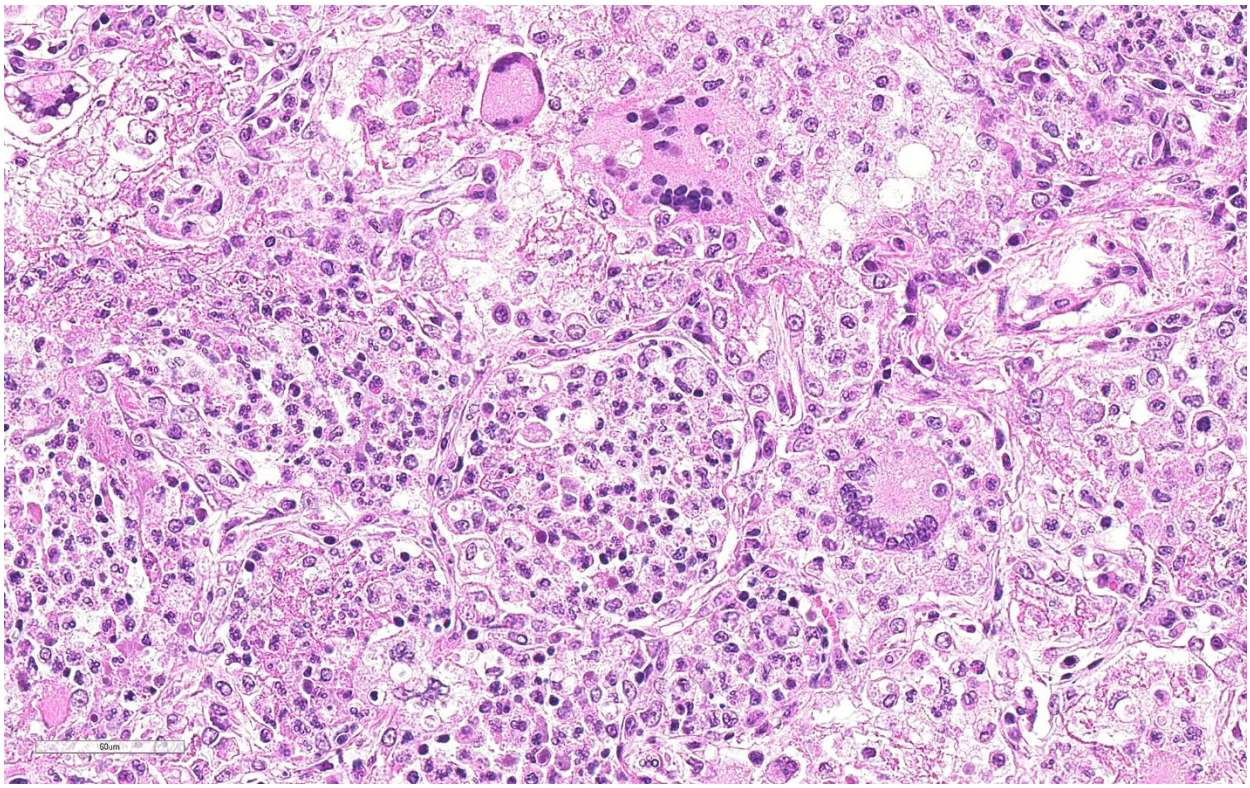

Lung, rhesus. Macrophages and neutrophils fill alveoli along with scattered viral syncytial giant cells. (HE, 400X)

is often an indication of terminal phase of disease progression.[7]

The most common pulmonary lesion in HIV is a lymphocytic and histiocytic pneumonia, centered around vessels and bronchioles.[6] Interestingly, when this syndrome occurs, HIV- infected individuals have lower incidence of opportunistic infections and longer survival times. SIV is similar, and macrophage-tropic strains cause pneumonia.[1,2,6]. If these infected macrophages go on to form giant cells, this is generally the terminal phase of SAIDS. If it infects macrophages and there is a T cell response in the lung, humans with the disease get pneumonia, but not OIs and death.

Pulmonary opportunistic infections in both AIDS patients and SAIDS-infected monkeys include *Pneumocystis carinii*, *Mycobacterium avium-intracellulare*, cytomegalovirus, *Cryptosporidium parvum* as well as other bacteria, fungal, and viral organisms. Pulmonary conditions reported to occur secondary to AIDS or SAIDS include Kaposi's sarcoma, nonspecific pneumonitis, pulmonary lymphoma, pulmonary lymphoid hyperplasia, and lymphocytic interstitial pneumonia. *Pneumocystis carinii* infection in macaques is characterized by foamy pink exudate within alveoli, extensive lymphocytic infiltration, and type II pneumocyte hyperplasia.[3]

Pulmonary multinucleate giant cells and histiocytic infiltrates have been observed in

SIV infected rhesus macaques.[7] Viral antigen (p26 and p14) has been observed on theses syncytial cells and smaller macrophages in alveolar spaces, circulating in pulmonary blood vessels, and in the sinusoids of tracheobronchial lymph nodes of moribund animals.[2] These cells have also been labeled with a-1-antichymotrypsin, indicating macrophage origin. This spectrum of lesions is seen in monkeys that are free from CMV.[2] The more common pulmonary change in SIV infection is perivascular mononuclear inflammation between 2-8 weeks after inoculation. SIV arrives at the lung hematogenously likely within lymphocytes or macrophages. This characteristic infiltrate of multinucleate giant cells reflects the final stage of disease where the immune system is unable to restrict viral replication in macrophages. Disseminated giant cell disease is a characteristic of terminal AIDS/SAIDS.[3,8]

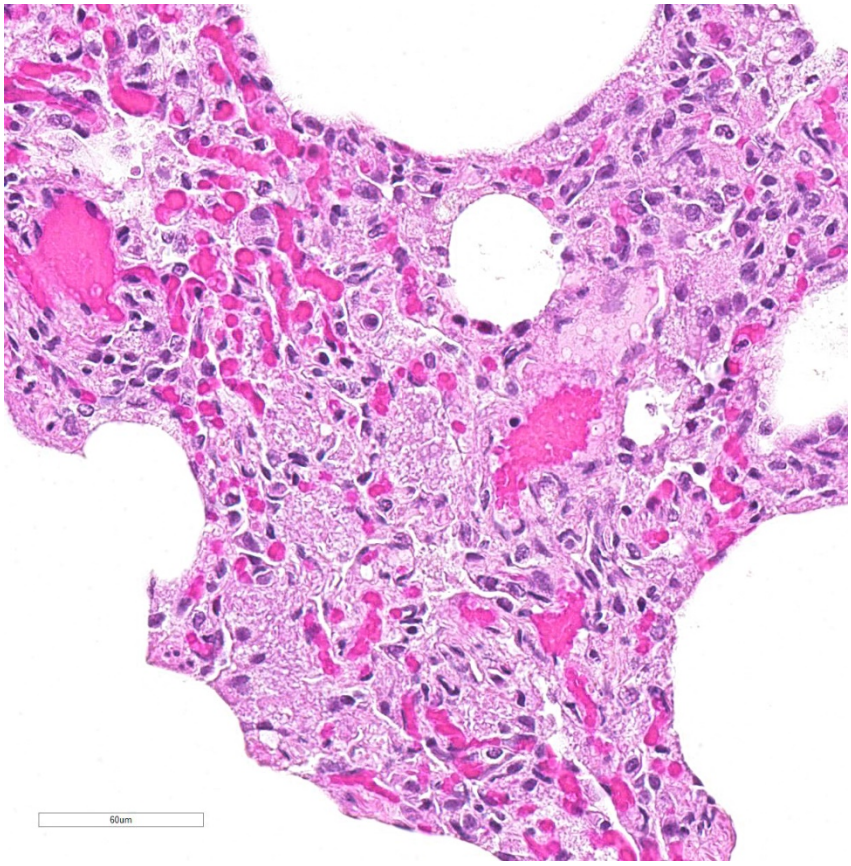

Lung, rhesus. In less damaged areas of the section, alveoli are filled with macrophages and eosinophilic flocculent protein. (HE, 400X).

Contributing Institution:

Harvard Medical School
Division of Comparative Pathology
New England Primate Research Center
One Pine Hill Drive
Southborough, MA 01772|
www.hms.harvard.edu/NEPRC

JPC Diagnosis: Lung: Pneumonia, interstitial, histiocytic, with abundant fungal cysts, neutrophils and numerous viral syncytia.

JPC Comment: The contributor provides a concise overview of pulmonary SIV infection in the macaque, which very closely approximates common events as seen in HIV infected humans.

The fungus *Pneumocystis carinii* was first identified in post-World-War II Europe in malnourished children, and prior to the onset of the HIV epidemic in the 1980s, was most

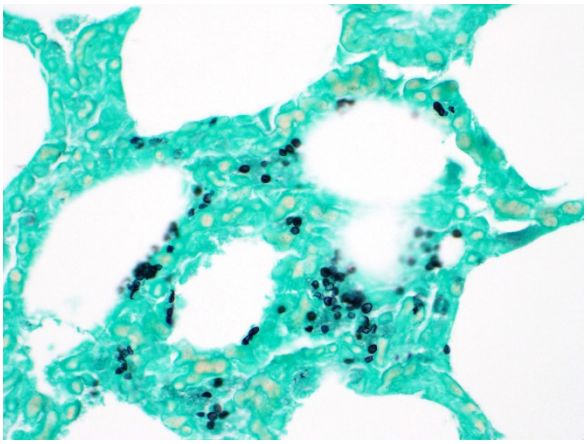

Lung, rhesus. Asca of Pneumocystis carinii are embedded in the flocculent proteinaceous exudate. (GMS, 400X).

often seen in patients undergoing chemotherapy. Infection elicits humoral and cell mediated responses in affected individuals with the $CD4^+$T-cell-driven response considered the most important in combating infection. Asci, or cystic forms, have beta-glucan within their cell wall, which is recognized by alveolar macrophages and epithelial which ultimately prime the T-cell response. Various inflammatory responses, including Th1, Th2, and Th17 responses all been identified in various cases of PCP, however, none have been shown to be intrinsic to disease clearance. Trophozoites, whch lack a cell wall, do not stimulate the response, and may actively inhibit it. Macrophages also appear to be the primary cell responsible for killing the fungus.

Coinfection by *Pneumocystis carinii* in SIV-infected macaques with AIDS is a common finding, especially in terminal stages of the disease. Experimental models of *Pneumocystis carinii* pneumonia (PCP) infection in rhesus macaques have been established via pulmonary airway inoculation of SIV-infected animals, which allows the ability to study the pathogenesis of PCP in immunosuppressed patients. Characteristic findings in this model parallels those seen in natural infection, with an initial increase in $CD8^+$ T cells in the lung and bronchiolo-alveolar lavage fluid of affected animals until they constitute over 90% of $CD3^+$ T-cells. Infiltration of neutrophils into the lung generally heralds the onset of clinical disease and are considered a major cause of pulmonary damage in PCP.

It was generally accepted for many years among SIV researchers that the African nonhuman primates, which infected with lentiviruses do not progress to AIDS, as characterized by $CD4^+$ depletion, opportunistic infections, and neoplasia. A 2009 paper by Pandrea et al[8] chronicled progressive SIV infection in African green monkeys, mandrills, sooty and black mangabeys, and HIV infection in baboons and chimpanzees. While the viral loads required to infect these species is considerably higher than required to infect Asian macaques, and potentially higher than natural infection, it may be wise to consider same- and cross-species infection with lentivirus a “persistently non-progressive” rather than “non-pathogenic” infection in these species.[8]

References:

1 Babas T, Vieler E, Hauer DA, Adams RJ, Tarwater PM, Fox K, Clements JE, Zink MC: Pathogenesis of SIV pneumonia: selective replication of

viral genotypes in the lung. Virology **287:** 371-381, 2001

2 Baskin GB, Murphey-Corb M, Martin LN, Soike KF, Hu FS, Kuebler D: Lentivirus-induced Pulmonary Lesions in Rhesus Monkeys (*Macaca mulatta*) Infected with Simian Immunodeficiency Virus. Vet Pathol **28:** 506-513, 1991

3 Baskin GB, Murphey-Corb M, Watson EA, Martin LN: Necropsy Findings in Rhesus Monkeys Experimentally Infected with Cultured Simian Immunodeficiency Virus (SIV)/Delta. Vet Pathol **25:** 456-467, 1988

4. Board KF, Patil S, Lebedeva I, CapuanoIII S, Trichel AM, Murphey-Corb M, Rajakumar PA, Flynn JL, Haidaris CG, Noris KA. Experimental Penumocystic carinii pneumonia in simian immunodeficiency virus-infected rhesus macaques. *J Inf Dis 2*003; 187:576-588.

5. Hoving JC, Kolls JK. New advances in understanding the host immune response to Pneumocystis. *Curr Opin Microbiol* 2017; 40:65-71

6. Mankowski JL, Carter DL, Spelman JP, Nealen ML, Maughan KR, Kirstein LM, Didier PJ, Adams RJ, Murphey-Corb M, Zink MC: Pathogenesis of Simian Immunodeficiency Virus Pneumonia. Am J of Pathol **153:** 1123-1130, 1998

7. McClure HM, Anderson DC, Fultz PN, Ansari AA, Lockwood E, Brodie A: Spectrum of disease in macaque monkeys chronically infected with SIV/SMM. Vet Immunol Immunop **21:** 13-24, 1989

8. Pandrea I, Silvestri G, Apetrei C: AIDs in African NHP hosts of SIVs: A New Paradigm of SIV Infection. Cur HIV Res **7:** 57-72, 2009

CASE III: WSC Case 2 HE (JPC 4118136).

Signalment2-year-old, intact male, Harlan Sprague-Dawley rat (*Rattus norvegicus)*

History: This rat was a terminal sacrifice (Test Day 730) animal from the control (untreated) group of a chronic, 2-year carcinogenicity study. No clinical signs or gross lesions were noted.

Gross Pathology: N/A

Laboratory results: N/A

Microscopic Description:

There is marked, irregular undulation along the capsular cortical surface. Diffusely throughout the cortex, there is moderate loss of renal tubules with replacement and wide separation of remaining tubules by abundant interstitial fibrous connective tissue, edema, and mixed inflammatory cells, including predominantly small lymphocytes and plasma cells. Low numbers of brown, granular pigment-laden (hemosiderin-laden) macrophages are also scattered throughout the cortical interstitium. Multifocal small

interstitial hemorrhages are also present. The majority of remaining renal tubules are moderately to marked dilated and vary from empty to often filled with eosinophilic proteinaceous fluid or protein (hyaline) casts. Occasionally, a few scattered tubules have sloughed, necrotic epithelial cells and/or small intraluminal clusters of degenerative neutrophils admixed with necrotic cellular and nuclear debris and rare erythrocytes. Renal tubular epithelial changes range from cytoplasmic swelling and vacuolization (degeneration) to attenuation and atrophy. The tubular basement membrane is often thickened and hyalinized. Frequent scattered regenerative tubules are also present. Regenerative tubules are lined by one or multiple layers of crowded, plump epithelium characterized by slight cytoplasmic basophilia and large, vesicular nuclei with a single prominent nucleolus and increased mitoses. Rarely, a small papillary projection of jumbled renal tubular epithelium projects into the lumen. The majority of glomeruli are enlarged with glomerular tufts segmentally to globally

Kidney, rat. Subgross changes include an irregular contour of the capsule, diffuse ectasia of tubules, protein casts and interstitial hypercellularity predominantly within the outer stripe of the medulla, and mild dilation of the renal pelvis. (HE, 7X)

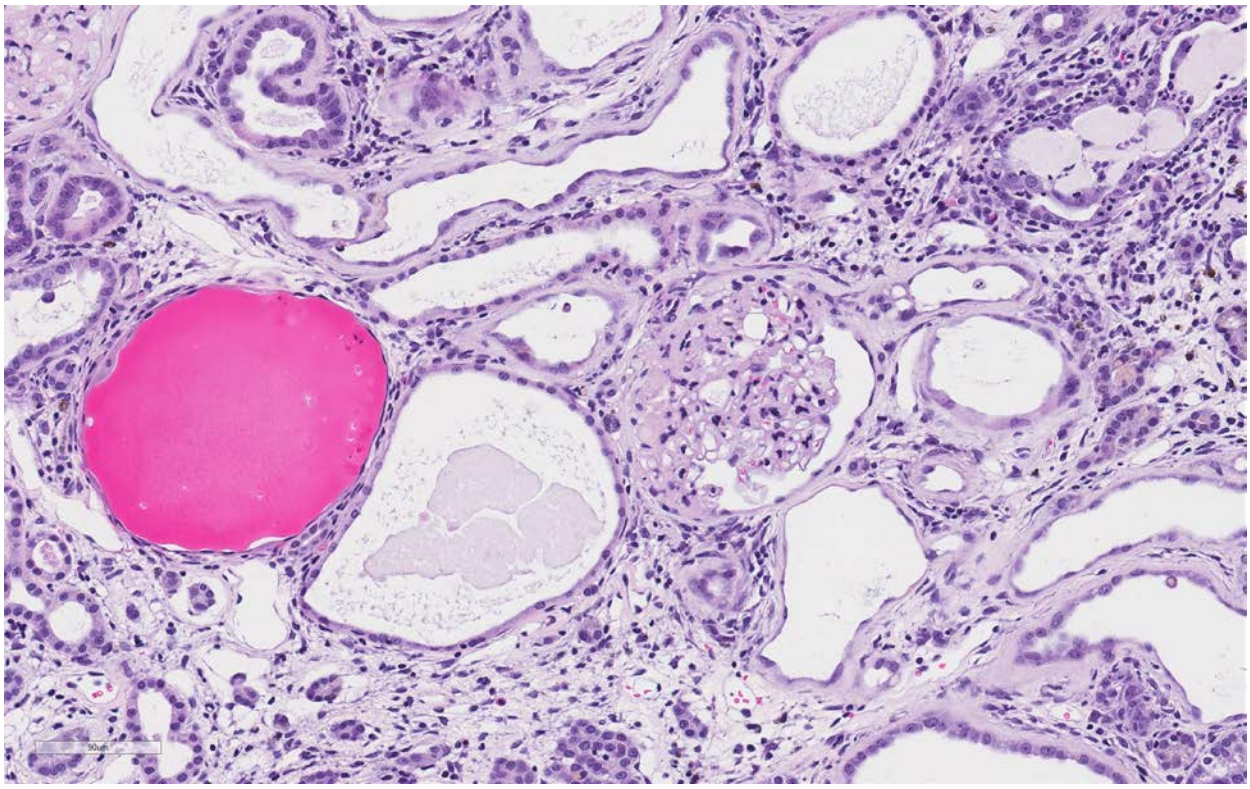

Kidney, rat. There is marked expansion of the interstitium with edema, collagen, and lymphocytes, plasma cells, and rare neutrophils. Tubules are markedly ectatic, often lined by attenuated epithelium, have a thickened basement membranes, and contain luminal protein. Other tubules within areas of fibrosis are shrunken and atrophic. The glomerulus at center has markedly thickened capillary basement membrane and early Synechiae formation approximately 50% around Bowman's membrane. (HE, 150X)

expanded by increased mesangial fibrous connective tissue, Bowman's capsule thickened and hyalinized, and periglomerular fibrosis (glomerulosclerosis). The parietal epithelium lining Bowman's capsule is often hypertrophied and glomerular tufts are multifocally adhered to Bowman's capsule (synechiae). The urinary space is often moderately dilated. A few shrunken, obsolescent glomeruli are also seen.

Contributor's Morphologic Diagnosis:

Kidney: Tubular degeneration, atrophy, necrosis, and regeneration, diffuse, severe with thickened basement membranes, tubular ectasia and hyaline casts, chronic interstitial nephritis and fibrosis, and glomerulosclerosis, segmental to global (chronic progressive nephropathy)

Contributor's Comment: Chronic progressive nephropathy (CPN) is very common in all conventional strains of laboratory rat, with the highest incidence and severity in the Fischer 344 and Sprague-Dawley strains.[2-4] The disease also occurs at a higher incidence and with progressively greater severity in male rats than in female rats.[2-4,6] CPN is also a very common spontaneous renal disease of aging laboratory mice.[3-4,6] A similar disease has been described in the gerbil, common marmoset, and naked mole rat. [5,6,8] In guinea pigs, segmented nephrosclerosis shares some features with CPN.[5]

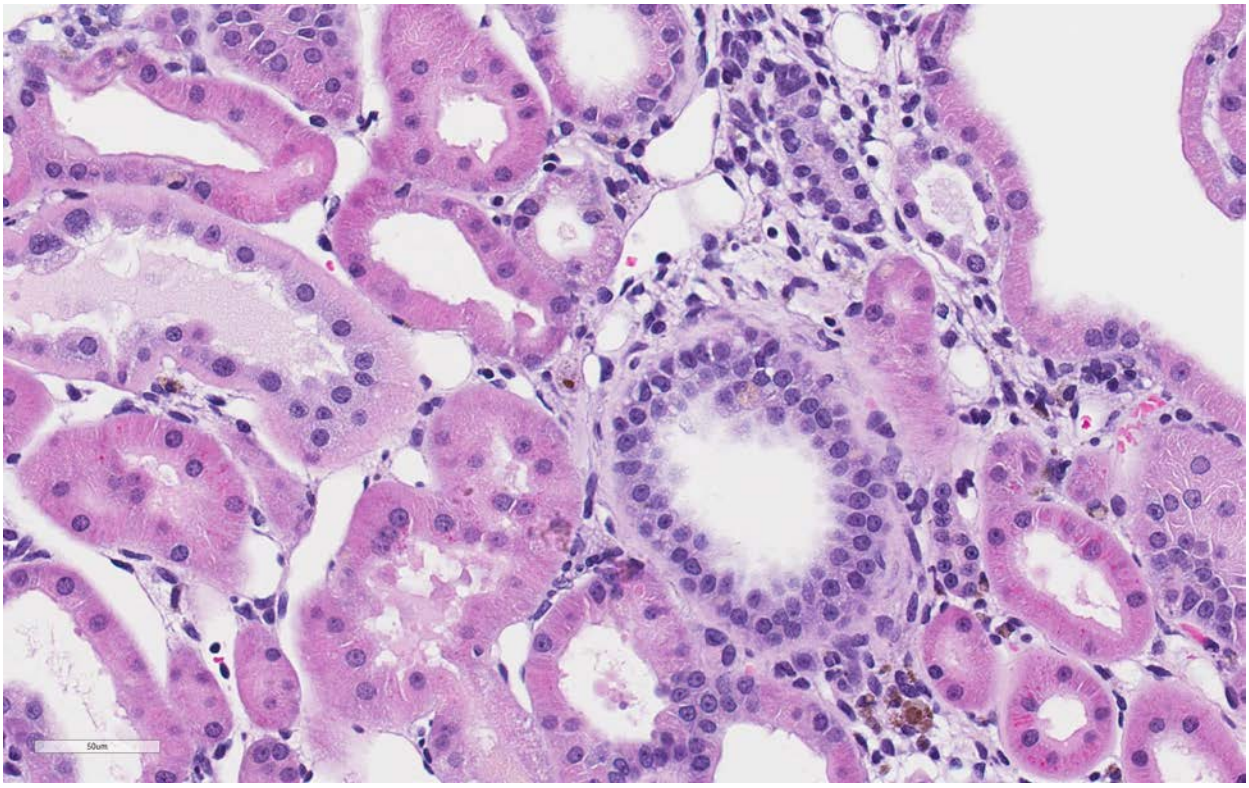

Liver, rat. Regenerating tubules are characterized by cytoplasmic basophilia and nuclear crowding. (HE, 276X)

CPN is a major cause of morbidity and mortality in laboratory rats.[3,4] Although commonly thought of as an aging disease, many rats start developing the earliest lesions of CPN as juveniles (2-3 months old).[3] The disease progresses throughout the life of the animal, eventually leading to end-stage renal disease in the rat.[2-4] Renal failure from CPN can sometimes account for up to 50% or more of unscheduled male rat deaths in chronic carcinogenicity bioassays.[3]

The cause of CPN is unknown[2-4], although Manskikh recently proposed a hypothesis for an expanding somatic mutant clone of precursor cells of tubular epithelium as the inciting cause.[6] A number of dietary and hormonal factors are known to influence the incidence and severity of disease. The primary diet-related factors of importance are total caloric intake as well as source and amount of protein in the diet. Restricting caloric intake and reducing protein in the diet can reduce the incidence and severity of CPN. With regard to hormonal factors, the sex predisposition of the disease is linked to the presence of androgens, rather than an absence of estrogen.[2-4]

Classically, the glomerulus has been thought to be the primary target, with hyperfiltration being the underlying basis for the pathogenesis.[3-5] This theory has been perpetuated due to the influence of high protein diets on disease progression and the associated clinical pathology finding of albuminuria in affected animals. However, this proposed glomerular hyperfiltration pathogenesis has not been proven; in fact, in aging rats, there is no evidence for a causal

relationship between glomerular capillary blood pressure and the structural damage to glomeruli, arguing against this theory of a primary hemodynamic mechanism.[4] Additionally, the earliest lesion of CPN that is detectable by light microscopy is actually a renal tubular lesion – a focal simple tubular hyperplasia of the P1 segment of a proximal tubule. This focal tubular lesion progresses to a small focus of affected tubules within a nephron and eventually to involve adjacent nephrons. Tubular basement membrane thickening is often a very prominent feature. Glomerular lesions generally develop later in the course of the disease.[2-4] However, it cannot be ruled-out that a functional alteration in the glomerulus which cannot be detected microscopically may occur prior to this tubular lesion. During later and more severe stages of the disease, CPN is predominantly characterized by both degenerative and regenerative tubular changes, including numerous protein casts, as well as prominent segmental to global glomerulosclerosis.[1-3] In severe grade cases, vesicular alteration of the renal papilla can be seen.[7] Deposition of interstitial extracellular matrix (fibronectin, thrombospondin, collagens I and III) and infiltration by mononuclear inflammatory cells is often seen as well but these components are generally mild and not prominent features of the disease.[1-3] Notably, vascular lesions are not a part of the disease.[3,4]

With regard to experimental studies and chronic carcinogenicity bioassays, some chemicals can induce exacerbation of CPN and, given the proliferative nature of the disease, advanced CPN is itself a risk factor for a marginal increase in the incidence of renal tubule tumors.[2-4] In humans, the most common renal diseases are diabetic nephropathy and hypertensive nephropathy. The biology and lesions of rat CPN do not mirror those of either of these nephropathies nor of any of the additional known, less common nephropathies of humans; there is no known counterpart of rat CPN in humans.[3] As such, there is debate over the conclusions that can be drawn from chronic carcinogenicity bioassays using rats regarding small increases in the incidence of renal tubule tumors and the relevance to human health. When designing experiments and interpreting the data from studies using the laboratory rat, relevance for species extrapolation to humans needs to be considered, particularly with regard to determining nephrotoxic effects and risk for renal tumor development.

Contributing Institution:

National Toxicology Program
National Institute of Environmental Health Sciences
111 TW Alexander Drive, PO Box 12233
Research Triangle Park, NC 27709

https://www.niehs.nih.gov/research/atniehs/labs/lep/ntp-path/index.cfm

JPC Diagnosis: Kidney: Nephritis, interstitial, chronic, diffuse, severe, with membranous glomerulonephritis, synechiae, tubular loss, degeneration, necrosis, and regeneration, and marked interstitial fibrosis.

JPC Comment: The contributor has provided an excellent review of chronic progressive nephropathy of rats (CPN), a

very common age-related finding in laboratory rodents, which may have an important and deleterious effect on analysis in chronic studies.

From a strain perspective, Sprague-Dawley and Fischer 344 appear to be the most affected by this condition, followed by Wistar, Long-Evans, and Brown Norway strains, with Buffalo and Osborne-Mendel the most resistant.[1] The changes are grossly apparent only in the later stages of disease, presenting as kidneys which are decreased in size with an irregular contour, and a golden, rather than brick-red coloration.

Microscopically, lesions may be seen as early as 2-3 months of age in male rats of predisposed strains as individual regenerative tubules within the cortex with basophilic cytoplasm, epithelial crowding, and an irregularly thickened basement membrane. Affected tubules will accumulate hyaline material in their lumen over time, predominantly in inner stripe of the outer medulla (descending loop of Henle). Over time, individual diseased and regenerative tubules become enlarging foci, hyaline casts extend into the cortex, and eosiniophlic droplets may be seen in tubular epithelium (most prominently in males). Visible glomerular changes develop at this time. Shortly, interstitial inflammation (beginning at the cortical medullary junction) and fibrosis develops.[1]

End stage CPN is characterized by involvement of the entire kidney and various effects in other organs: hyperplasia of the chief cells of the parathyroid gland as well as metastatic calcification in a number of organs, including the kdney, lung, media of large arteries, and the gastrointestinal tract. An additional lesion of end-stage CPN, which may be overlooked with the myriad and severe changes of the glomeruli, tubules, and interstitium, is papillary hyperplasia of the epithelium of the renal pelvis. This lesion consistst of projections of hyperplastic transitional epithelium containing large dilated vessels which project into the pelvic lumen.[1]

Clinicopathologic findings in affected animals include marked proteinuria and aluminuria and resulting hypoproteinemia, hypoalbuminemia, and hypercholesterolemia, demonstrating the severity of the glomerular damage. Decreased functional renal mass results in hyperphosphatemia, and serum calcium is decreased as a result of Starling's law as well as hypoalbuminemia. Serum nitrogen and creatinine values increase only in late stages of the disease.[1]

References:

1. Seely JC, Hard GC, Blankenship B. Urinary Tract. *In: Boorman's Pathology of the rat: reference and atlas, 2nd edition,* Suttie A, Leininger JR, Bradley AE, eds. London, Academic Press 2018; pp 135-137.
2. Hard GC, Banton MI, Bretzlaff RS, et al. Consideration of Rat Chronic Progressive Nephropathy in Regulatory Evaluations for Carcinogenicity. *Toxicol Sci*. 2013;132(2): 268-275.
3. Hard GC, Johnson KJ, Cohen SM. A comparison of rat chronic progressive nephropathy with human renal disease –

implications for human risk assessment. *Crit Rev Toxicol*. 2009;39(4):332-346.
4. Hard GC, Khan KN. A Contemporary Overview of Chronic Progressive Nephropathy in the Laboratory Rat, and Its Significance for Human Risk Assessment. *Toxicol Path*. 2004;32:171-180.
5. Manskikh VN. Hypothesis: Chronic Progressive Nephropathy in Rodents as a Disease Caused by an Expanding Somatic Mutant Clone. *Biochemistry Moscow*. 2015;80(5):689-693.
6. Manskikh VN, Averina OA, Nikiforova AI. Spontangenous and Experimentally Induced Pathologies in the Naked Mole Rat (*Heterocephalus glaber*). *Biochemistry Moscow*. 2017;82(12):1504-1512.
7. Souza NP, Hard GC, Arnold LL, Foster KW, Pennington KL, Cohen SM. Epithelium Lining Rat Renal Papilla: Nomenclature and Association with Chronic Progressive Nephropathy (CPN). *Toxicol Path.* 2018;46(3):266-272.
8. Yamada N, Sato J, Kanno T, Wako Y, Tsuchitani M. Morphological Study of Progressive Glomerulonephropathy in Common Marmosets (*Callithrix jacchus*). *Toxicol Path*. 2013;41:1106-1115.

CASE IV: L19-3350 (JPC 4135947).

Signalment: 7-year-old, intact female, Flemish giant domestic rabbit (*Oryctolagus cuniculus*)

History: The rabbit presented with a 1-month history of severe subcutaneous swelling, erythema, ulceration and abscess formation of the left hindlimb extending from the hock to the digits. A focal area of mild subcutaneous swelling was also noted on the plantar surface of the right hindlimb metatarsal area with a similar exudate on cut surface. The animal was housed on a wire cage outdoors with no bedding. Decreased borborygmi were noted on auscultation and the haircoat in the perineal region was stained with feces. Due to the severity of the lesions, which would require limb amputation, euthanasia was elected.

Gross Pathology: The left metatarsal region is markedly swollen, with multifocal ulceration and fistulous tracts that extend to

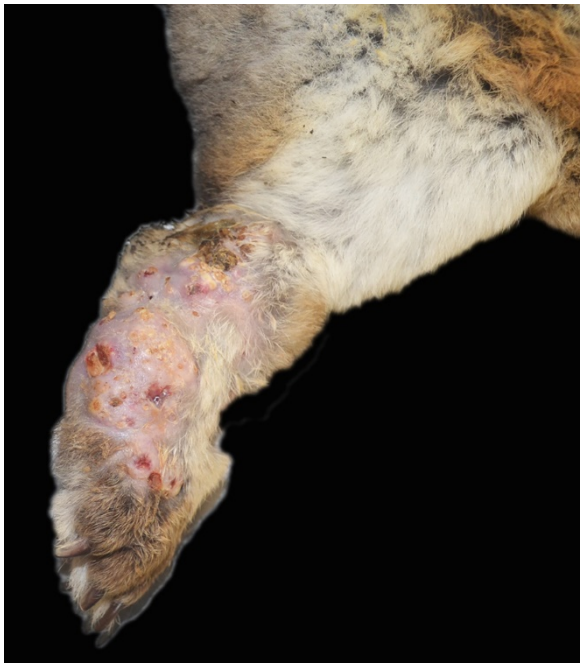

Metatarsus, rabbit The left metatarsal region is swollen, with multifocal ulceration and fistulous tracts. (Photo courtesy of: Louisiana Animal Disease Diagnostic Laboratory (LADDL), School of Veterinary Medicine, Louisiana State University (http://www1.vetmed.lsu.edu/laddl/index.html)

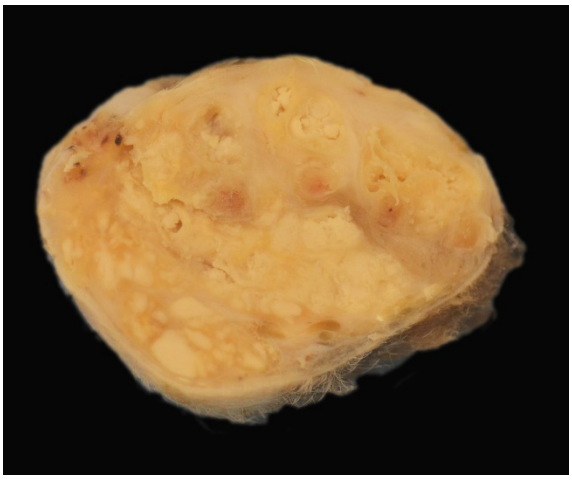

Metatarsus, rabbit. Multifocal abscesses containing abundant, inspissated, white to pale yellow, granular exudate are seen on cut surface. (Photo courtesy of: Louisiana Animal Disease Diagnostic Laboratory (LADDL), School of Veterinary Medicine, Louisiana State University (http://www1.vetmed.lsu.edu/laddl/index.html)

the plantar surface of the paw On cut surface, the subcutis is effaced by multifocal abscesses containing abundant, inspissated, white to pale yellow, granular exudate extending to the periosteum of the underlying metatarsal and phalangeal bones.The distal right metatarsal region has a 0.5 cm diameter focal abscess within the subcutis.

Laboratory results: Bacteriology: Skin – Moderate growth of *Pseudomonas aeruginosa*

Microscopic Description:

Haired skin (left distal hindlimb): The dermis and panniculus are effaced by multifocal to coalescing areas of liquefactive necrosis characterized by abundant hypereosinophilic cellular debris, hemorrhage, numerous heterophils and colonies of coccobacillary bacteria surrounded by abundant intensely eosinophilic (hyalinized) material frequently forming radiating, club-like projections (Splendore-Hoeppli reaction). The areas of necrosis are peripherally delimited by abundant foamy histiocytes and proliferation of dense fibrous connective tissue. There are occasional dilated lymphatic vessels. The cortical bone of the metatarsal and phalangeal bones represented in the sections have variable areas of periosteal bone proliferation and occasional Howship's lacunae containing osteoclasts. Other histologic changes variably represented in the sections include proliferation of the synovial membrane within tendon sheaths along with moderate infiltration of lymphocytes and plasma cells; skeletal muscle atrophy, regeneration and replacement by fibrous connective tissue characterized by shrunken myofibers, multinucleated myocytes and moderate endomysial infiltration of lymphocytes and plasma cells; and peripheral nerve fiber degeneration and loss characterized by marked vacuolization and deposition of mucinous matrix and/or fibrous connective tissue within the endoneurium. Histologic changes within the epidermis and adnexa are also variably represented in the

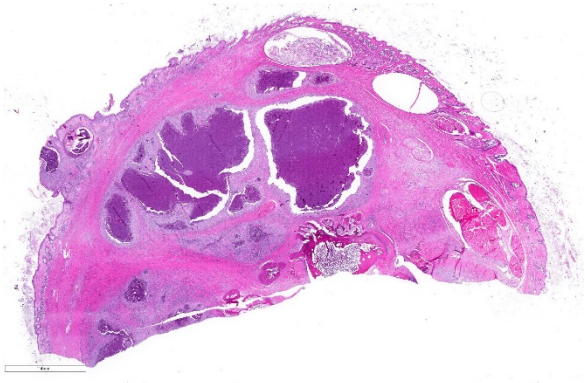

Partial cross section, metatarsus. Within the deep dermis, focally extending to the epidermis and abutting the bone, there are numerous multifocal to coalescing pyogranulomas. There is a proliferative reaction arising from the cortex of the underlying bone. (HE, 7X)

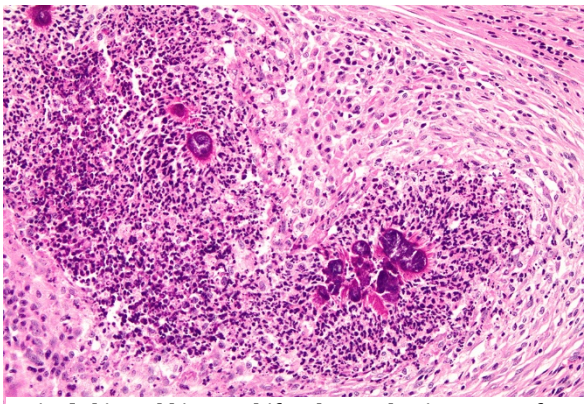

Haired skin, rabbit. Multifocal to coalescing areas of necrosis with numerous colonies of bacteria delimited by abundant Splendore-Hoeppli reaction. (HE, 200X) (Photo courtesy of: Louisiana Animal Disease Diagnostic Laboratory (LADDL), School of Veterinary Medicine, Louisiana State University (http://www1.vetmed.lsu.edu/laddl/index.html)

sections. The epidermis is markedly hyperplastic with occasional pustules and crusts, and multifocal transepidermal elimination of necrotic debris and bacterial colonies into the epidermal surface or into the lumen of hair follicles is also noted (Figure 4). Multiple hair follicles are markedly dilated and filled with abundant keratin (comedone), and the adnexa are frequently delimited by moderate numbers of lymphocytes and plasma cells. Special stains performed (Gram, Gridley, Giemsa, Steiner, and Fite's) characterized bacterial colonies as being composed by short rod-shaped gram-negative bacteria that also stain strongly basophilic with Giemsa (Figures 5 and 6). No fungal organisms, spirochetes or acid-fast bacteria were identified.

Additional histologic findings (not represented in the sections) include marked myeloid hyperplasia with a left shift, mild to marked extramedullary hematopoiesis in the liver and spleen, and abundant intravascular heterophils within pulmonary capillaries and larger vessels.

Contributor's Morphologic Diagnosis:

Skin (left distal hindlimb): Dermatitis and panniculitis, pyogranulomatous, multifocal to coalescing, severe, with abundant large intralesional gram-negative bacterial colonies and Splendore-Hoeppli reaction.

Contributor's Comment: Botryomycosis, also known as bacterial pseudomycetoma, is a term that commonly refers to a chronic bacterial infection of the skin and subcutis caused by non-filamentous bacteria that tend to form grossly visible colonies as tissue grains within the lesions (noted in this case as a granular exudate).[11] This condition affects multiple animal species including equids, cattle, dogs, hamsters, mice, rats, rabbits and guinea pigs.[1-6,9,12,14-16] It has to be differentiated from actinomycotic and eumycotic mycetomas, which usually present with similar gross and histologic lesions. Actinomycotic mycetomas are frequently associated with subcutaneous *Actinomyces* spp. or *Nocardia* spp. infections, which can be differentiated histologically using special stains including Gram and modified acid-fast: *Actinomyces* spp. are gram-positive, non-acid-fast, filamentous bacteria, and *Nocardia* spp. are gram-positive and variably acid-fast filamentous bacteria. Eumycotic mycetomas are caused by a variety of fungi that can be readily identified using stains such as methenamine silver.

Botryomycotic lesions usually develop in the skin and subcutis, but frequently extend deeply, affecting the underlying muscle and bone. Visceral lesions are uncommon but have been reported in multiple species as well.[2,4,15] Grossly, lesions are characterized

by firm, focal to multifocal nodules containing a white to yellow exudate with a gritty texture (tissue grains) that tend to ulcerate and/or develop fistulous tracts as observed in this case. Additional histologic findings in this rabbit included marked myeloid hyperplasia with a left shift, mild to marked extramedullary hematopoiesis in the liver and spleen, and abundant intravascular heterophils within pulmonary capillaries and larger vessels; all of these most likely related to the inflammatory response secondary to the infection.

The Splendore-Hoeppli phenomenon has been reported as a classic histologic feature of botryomycosis. Although its composition is not fully characterized, it is reportedly

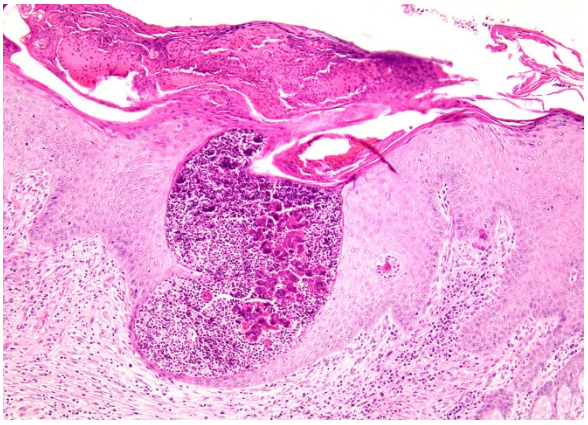

Haired skin, rabbit. The epidermis has multifocal areas of transepidermal elimination of necrotic debris and bacterial colonies and superficial serocellular crusts. (HE, 100X) (Photo courtesy of: Louisiana Animal Disease Diagnostic Laboratory (LADDL), School of Veterinary Medicine, Louisiana State University (http://www1.vetmed.lsu.edu/laddl/index.html)

composed of necrotic debris and deposition of immune complexes.[8] While in some cases deposition of immunoglobulins was observed via immunohistochemistry and immunoelectron microscopy, in other instances this material may be composed of eosinophilic major basic protein.[8,13] Differences in composition may be associated with the specific causative agent and probably other factors such as disease stage and previous treatments.[8]

Even though the pathogenesis of botryomycosis is not well understood, it is believed that the pyogranulomatous inflammation develops as a consequence of the complex interactions between the host response and the agent's virulence factors. It is speculated that the inability to clear the infection may be associated with a polysaccharide coating synthesized by the bacteria. Coagulase-positive staphylococci (mainly *S. aureus*) are the most common causative agents of botryomycosis, but other bacteria including *Pseudomonas* spp., *Streptococcus* spp., *Actinobacillus* spp., *Pasteurella* spp., *Proteus* spp., *Escherichia coli*, *Trueperella* spp. and *Bibersteinia* spp. have also been identified. This condition is generally secondary to wound contamination or traumatic lesions; in this case it was likely associated with poor housing conditions with no bedding. Usually, the bacteria are not well recognizable on H&E sections, in which special stains can aid in ruling out actinomycotic bacteria (actinomycotic mycetoma) and fungi (eumycotic mycetoma). Bacterial and/or fungal culture is required in order to confirm the etiologic agent. In this case, bacterial colonies were gram negative and basophilic with a Giemsa stain, consistent with the culture of *Pseudomonas aeruginosa*. The Gram and

Giemsa stains highlighted the radiating, club-like projections within the Splendore-Hoeppli material.

Contributing Institution:

Louisiana Animal Disease Diagnostic Laboratory (LADDL), School of Veterinary Medicine, Louisiana State University (http://www1.vetmed.lsu.edu/laddl/index.html)

JPC Diagnosis: Partial cross section of leg: Dermatitis and cellulitis, pyogranulomatous (heterophilic and granulomatous), multifocal to coalescing, severe, with Splendore-Hoeppli material and numerous bacilli.

JPC Comment: The contributor has provided an excellent review of the condition of botryomycosis, a unique histologic lesion that may be seen in a variety of species and tissues, and results from several common bacterial genera as mentioned by the contributor. It should be stressed that while Splendore-Hoeppli material, which may be composed of immunoglobulins, major basic protein, or both is a component of botryomycotic lesions, it may be seen in a number of other lesions other than botryomycosis, including many fungal and helminth infections, as well as surrounding a variety of inert materials within the skin and subcutis.[8]

Pseudomonas aeruginosa is a ubiquitous gram-negative organism of soil and aquatic environments, which, as a result of its intrinsic and expanding antibiotic resistance,

Haired skin, rabbit. Bacterial colonies are gram-negative. The Gram stain intensely highlights the club-like projections typical of the Splendore-Hoeppli reaction. (Gram, 400X) (Photo courtesy of: Louisiana Animal Disease Diagnostic Laboratory (LADDL), School of Veterinary Medicine, Louisiana State University (http://www1.vetmed.lsu.edu/laddl/index.html)

is a particulary worrisome opportunistic wound invader. It is a common opportunist in hospital settings, and the second most common isolate in ventilator-related infection.[5]

P. aeruginosa is a potent infectious agent in acute infections (with a host of virulence factors) and chronic infections (which are facilitated by its formation of biofilms). The bacterium possess flagella and type 4 pili, which provide a means of motility and cellular adhesion respectively, but also can stimulate an inflammatory response.[5] Like many other pathogenic gram-negative bacilli, it possesses a Type 3 secretion system, a needle-like evolutionary flagellar derivative, which allows it to inject exotoxins directly through a pore in the cell membrane. It possesses four exotoxins –

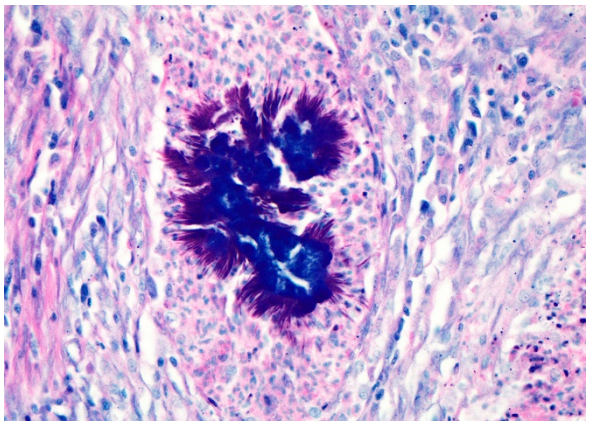

Haired skin, rabbit. Bacterial colonies are intensely basophilic on a Giemsa stain. Club-like projections typical of the Splendore-Hoeppli reaction are also highlighted. (Giemsa, 400X) (Photo courtesy of: Louisiana Animal Disease Diagnostic Laboratory (LADDL), School of Veterinary Medicine, Louisiana State University (http://www1.vetmed.lsu.edu/laddl/index.html)

exoU, exoS, exoS, and exoY – although often not all. ExoS has a deleterious effect on the actin cytoskeleton and exoU is a potent phospholipase. [5]

Chronic infections in wounds, burns, and ventilator-assisted patients (particularly patients with cystic fibrosis who are often immunosuppressed) are largely mediated by *P. aeruginosa*'s ability to create biofilms.[10] Biofilms are highly structured communities attached to each other and a surface, and act as a single unit directed by the secretion of diffusible molecules called autoinducers by dominant bacilli in their midst. Pathogenic strains of *Pseudomonas aeruginosa* produce three autoinducers which help organize biofilms in a variety of situations. [10]

One of the most deleterious effects of biofilms is the diffusional resistance they provide against antimicrobials and some autoinducers upregulate the production of beta-lactamases by *P. aeruginosa*, deactivating beta lactam antibiotics on the surface of the biofilm before they can diffuse into its depths. Moreover, biofilms protect their community from humoral aspects of immunity such as antibodies as well as impairing phagocytosis by their sheer size.[10]

References:

1. Akiyama H, Kanzaki H, Tada J, Arata J. Staphylococcus aureus infection on cut wounds in the mouse skin: experimental staphylococcal botryomycosis. *J Dermatol Sci.* 1996;11(3)**:**234-238.

2. Bostrom RE, Huckins JG, Kroe DJ, Lawson NS, Martin JE, Ferrell JF, et al. Atypical fatal pulmonary botryomycosis in two guinea pigs due to Pseudomonas aeruginosa. *J Am Vet Med Assoc.* 1969;155(7)**:**1195-1199.

3. Bridgeford EC, Fox JG, Nambiar PR, Rogers AB. Agammaglobulinemia and Staphylococcus aureus botryomycosis in a cohort of related sentinel Swiss Webster mice. *J Clin Microbiol.* 2008;46(5)**:**1881-1884.

4. Casamian-Sorrosal D, Fournier D, Shippam J, Woodward B, Tennant K. Septic pericardial effusion associated with pulmonary and pericardial botryomycosis in a dog. *J Small Anim Pract.* 2008;49(12)**:**655-659.

5. Gellatly SL, Hancock REW. Pseudomonas aeruginosa: new insights into pathogenesis and host

defenses. *Pathog Dis* 2013: 67:159-173.

6. Grosset C, Bellier S, Lagrange I, Moreau S, Hedley J, Hawkins M, et al. Cutaneous Botryomycosis in a Campbell's Russian Dwarf Hamster (Phodopus campbelli). *J Exotic Pet Med.* 2014;23(4)**:**389-396.

7. Hedley J, Stapleton N, Priestnall S, Smith K. Cutaneous Botryomycosis in Two Pet Rabbits. *J Exotic Pet Med.* 2019;28(1)**:**143-147.

8 Hussein MR. Mucocutaneous Splendore-Hoeppli phenomenon. *J Cutan Pathol.* 2008;35(11)**:**979-988.

9. Loader H, Lawrence KE, Brangenburg N, Munday JS. Cutaneous botryomycosis in a crossbred domestic pig. *N Z Vet J.* 2018;66(4)**:**216-218.

10. Mulcahy LR, Isabella VM, Lewis K. Pseudomonas aeruginosa biofilms in disease. *Microb Ecol* 2017

11. Padilla-Desgarennes C, Vazquez-Gonzalez D, Bonifaz A. Botryomycosis. *Clin Dermatol.* 2012;30(4)**:**397-402.

12. Percy DH, Barthold SW. *Pathology of Laboratory Rodents and Rabbits*. Ames, IA: Blackwell Publishing, 2007.

13. Read RW, Zhang J, Albini T, Evans M, Rao NA. Splendore-Hoeppli phenomenon in the conjunctiva: immunohistochemical analysis. *Am J Ophthalmol.* 2005;140(2)**:**262-266.

14. Shapiro RL, Duquette JG, Nunes I, Roses DF, Harris MN, Wilson EL, et al. Urokinase-type plasminogen activator-deficient mice are predisposed to staphylococcal botryomycosis, pleuritis, and effacement of lymphoid follicles. *Am J Pathol.* 1997;150(1)**:**359-369.

15. Share B, Utroska B. Intra-abdominal botryomycosis in a dog. *J Am Vet Med Assoc.* 2002;220(7)**:**1025-1027, 1006-1027.

16. Shults FS, Estes PC, Franklin JA, Richter CB. Staphylococcal botryomycosis in a specific-pathogen-free mouse colony. *Lab Anim Sci.* 1973;23(1)**:**36-42.